



ELSEVIER

Available online at www.sciencedirect.com

SCIENCE @ DIRECT®

Proceedings of the Combustion Institute 30 (2005) 439–446

Proceedings
of the
Combustion
Institute

www.elsevier.com/locate/proci

Computational and experimental study of JP-8, a surrogate, and its components in counterflow diffusion flames

James A. Cooke^a, Matteo Bellucci^a, Mitchell D. Smooke^{a,*},
Alessandro Gomez^{a,*}, Angela Violi^b, Tiziano Faravelli^c, Eliseo Ranzi^c

^a *Yale Center for Combustion Studies, Yale University, New Haven, CT 06520, USA*

^b *Department of Fuels and Chemical Engineering, University of Utah, Salt Lake City, UT 84112, USA*

^c *CMIC-Dipartimento di Chimica, Materiali ed Ingegneria Chimica, Politecnico di Milano, 20131 Milan, Italy*

Abstract

Non-sooting counterflow diffusion flames have been studied both computationally and experimentally, using either JP-8, or a six-component JP-8 surrogate mixture, or its individual components. The computational study employs a counterflow diffusion flame model, the solution of which is coupled with arc length continuation to examine a wide variety of inlet conditions and to calculate extinction limits. The surrogate model includes a semi-detailed kinetic mechanism composed of 221 gaseous species participating in 5032 reactions. Experimentally, counterflow diffusion flames are established, in which multicomponent fuel vaporization is achieved through the use of an ultrasonic nebulizer that introduces small fuel droplets into a heated nitrogen stream, fostering complete vaporization without fractional distillation. Temperature profiles and extinction limits are measured in all flames and compared with predictions using the semi-detailed mechanism. These measurements show good agreement with predictions in single-component *n*-dodecane, methylcyclohexane, and iso-octane flames. Good agreement also exists between predicted and measured variables in flames of the surrogate, and the agreement is even better between the experimental JP-8 flames and the surrogate predictions.

© 2004 The Combustion Institute. Published by Elsevier Inc. All rights reserved.

Keywords: Surrogate; JP-8; Simulation; Counterflow diffusion flames

1. Introduction

The study of the combustion processes in practical aero-combustors is an essential tool to characterize and improve combustor efficiency and to

identify and eliminate those mechanisms leading to pollutant formation. However, the numerical and experimental study of these processes in practical situations is daunting from two perspectives. The first challenge stems from the fact that aviation fuels, such as JP-8 and kerosene, are mixtures of a large number of hydrocarbons that together must meet standardized specifications. Due to the variability of composition, kinetic studies of such fuels can only be based on a “surrogate” mixture of well-known hydrocarbons that

* Corresponding authors. Fax: +1 203 432 6775 (M.D. Smooke); +1 203 432 7654 (A. Gomez).

E-mail addresses: mitchell.smooke@yale.edu (M.D. Smooke), alessandro.gomez@yale.edu (A. Gomez).

possesses thermochemical properties similar to those of the fuel under study. The kinetic mechanisms that describe such surrogate mixtures often consist of hundreds of gaseous species participating in thousands of reactions. From a computational perspective, these large mechanisms increase both the size and complexity of an already stiff set of strongly coupled, highly non-linear partial differential equations. A second challenge arises from the fact that combustion in practical aero-combustors, whether non-premixed or partially premixed, is certainly turbulent and inherently multidimensional. By some estimates, the direct numerical simulation (DNS) of turbulent combustion will exceed computational capabilities for at least 20 years [1]. However, there are computationally feasible alternatives that give substantial insight into the chemical and physical processes in turbulent flames while also allowing for the examination of complex chemistry and detailed transport in numerically and experimentally tractable configurations. One such configuration is the counterflow diffusion flame, an established tool with which to examine the interactions between detailed transport and complex chemistry, and one that affords good opportunities for comparison between computation and experiment.

A number of investigations have addressed the challenge of formulating surrogate blends for aviation fuels and developing the necessary kinetic mechanisms for these blends. The oxidation of these multicomponent mixtures has been studied computationally and experimentally in jet-stirred reactors for both two-component [2,3] and three-component surrogate mixtures [4] and in rich, premixed flames for a two-component surrogate mixture [3,5,6]. In contrast, there exist relatively few computational or experimental studies of the combustion of aviation fuels under non-premixed conditions. One recent example examines a counterflow kerosene diffusion flame computationally using a detailed kinetic mechanism for a two-component surrogate mixture [3].

As part of a broader effort to validate chemical kinetic models of multicomponent surrogates in a variety of combustion environments, we examine counterflow diffusion flames computationally and experimentally using both a six-component JP-8 surrogate blend and individual surrogate components as fuels. Experimentally, a non-sooting diffusion flame is stabilized between counter-flowing, nitrogen-diluted streams of fuel and oxygen. Temperature profiles and extinction limits are measured for each flame and are compared against predicted values obtained using a two-point boundary value solver and a semi-detailed kinetic model developed for the six-component surrogate. Preliminary results were presented in [7].

2. The surrogate

The present study models JP-8 as a six-component blend of well-known hydrocarbons with the following molar composition: 10% iso-octane (C_8H_{18}), 20% methylcyclohexane (C_7H_{14}), 15% *m*-xylene (C_8H_{10}), 30% *n*-dodecane ($C_{12}H_{26}$), 5% tetralin ($C_{10}H_{12}$), and 20% tetradecane ($C_{14}H_{30}$). This surrogate blend accurately simulates the volatility and smoke point of a practical JP-8 fuel [8]. The semi-detailed kinetic mechanism for this surrogate blend is based on an existing hierarchically constructed kinetic model for alkanes and simple aromatics extended to account for the presence of tetralin and methylcyclohexane as reference fuels [8,9]. This mechanism has been previously validated by comparing numerical simulations with experimental results for individual surrogate components in plug flow reactors and rich premixed flames as well as with experimental data for rich, premixed kerosene flames [8].

3. Numerical methods

We use the elliptic form of the two-dimensional conservation equations to model the gas-phase counterflow diffusion flame, shown schematically in the inset of Fig. 1. The result is a strongly coupled, highly non-linear set of $K + 4$ partial differential equations in cylindrical coordinates, where K is the number of gas-phase species. A similarity solution valid along the stagnation streamline reduces the complexity of the problem [10]. This assumption reduces the set of non-linear partial differential equations in two dimensions to a set of non-linear ordinary differential equations valid along the stagnation streamline. The problem is then closed with the ideal gas law and the application of appropriate boundary conditions, including a plug flow velocity boundary condition at both inlets. Local properties are evaluated using vectorized and highly optimized transport and chemistry libraries [11].

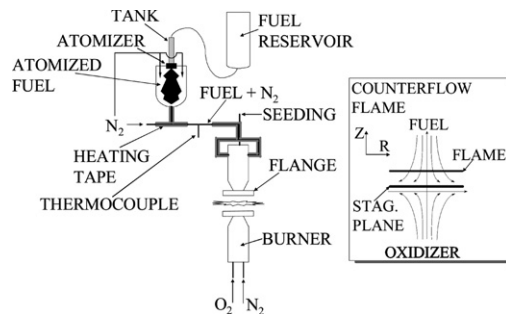


Fig. 1. A schematic diagram of the experimental setup, with an inset diagram of the counterflow diffusion flame.

The study uses a semi-detailed kinetic mechanism developed for the six-component JP-8 surrogate mixture described above, resulting in 221 gas-phase species participating in 5032 reversible reactions [8]. The effect of gas-phase radiation in the optically thin limit is considered by including a radiation submodel in which H₂O, CO, and CO₂ are the significant radiating species [12].

The solution of the governing equations proceeds with an adaptive non-linear boundary value method. The details of this method have been presented elsewhere [13,14], and only the essential features are outlined here. With the continuous differential operators replaced by finite difference expressions, the problem of finding an analytical solution to the governing equations is converted to one of finding an approximation to the solution at each mesh point. This set of $K + 4$ coupled difference equations is solved using a modified Newton's method in which the numerical Jacobian is periodically re-evaluated. Pseudo-transient continuation is employed to ease convergence of a starting estimate on an initial grid. The final computational grid is obtained adaptively through the equidistribution of the solution gradient and curvature between adjacent mesh points [15].

Once a solution is obtained for the governing equations with a given set of inlet conditions, the adaptive boundary value solver is coupled with arc length continuation [16,17] to obtain efficient and accurate solutions across a wide range of inlet conditions. Specifically, we use individual inlet variables as bifurcation parameters to examine a variety of inlet velocities and to manipulate inlet composition to separate the individual surrogate components. The ability of the arc length continuation algorithm to identify and traverse turning points in solution space facilitates the calculation of extinction limits.

4. Experimental methods

A schematic of the experimental setup is shown in Fig. 1. We have designed a counterflow burner using carefully contoured geometries to ensure flow uniformity at the burner mouths. Experiments have been conducted with a fuel mixture introduced from the upper burner, to benefit from the heating of the exhaust gas and to reduce the risk of condensation, and an oxidizer mixture introduced from the lower burner. The fuel and oxidizer inlet concentrations are chosen to inhibit the formation of soot, resulting in an overall fuel-lean flame. The fuel side is maintained at a temperature above the dew point of the nitrogen-diluted fuel mixture admitted into the burner. The flow rates of the reactant streams have been measured using calibrated rotameters.

The vaporization of the liquid fuel is a critical issue. For a single-component fuel, it is sufficient

to bubble inert through an evaporator maintained at an elevated and uniform temperature by a heated fluidized bed [7]. For the multicomponent mixture, such a system is susceptible to fractional distillation, especially if the volatilities of the components differ significantly, as in the present case. To circumvent these difficulties, an ultrasonic nebulizer (Aerogen), capable of generating rapidly vaporizing droplets of a few microns in diameter, has been used to introduce liquid fuel droplets into a heated nitrogen stream, yielding complete vaporization without fractional distillation. This vaporized fuel/inert mixture is then conveyed to the burner through a tube maintained at elevated temperature and monitored via thermocouples.

Temperature measurements are obtained using a coated Pt/10% Pt–Rh thermocouple with a wire diameter of 190 μm . The thermocouples are coated with SiO₂ to minimize catalytic effects and are replaced frequently to mitigate the effects of crack development in the coating. Thermocouple measurements are corrected for radiative losses both spherically and cylindrically. The thermocouple probe has been custom designed to minimize perturbations on the low strain velocity field.

The extinction limit for a given flame is measured by fixing the fuel inlet conditions and slowly decreasing the oxygen content of the oxidizer stream while simultaneously increasing the inert flow rate, with the total flow rate at the oxidizer inlet fixed, until instantaneous extinction is observed. The uncertainty regarding the extinction oxygen mole fractions is estimated at $\pm 10\%$ of the quoted limit.

5. Results and discussion

The mechanism validation efforts presented in this study proceed hierarchically, with the submodels for individual surrogate components validated prior to the examination of the surrogate blend. However, experimental considerations related to the toxicity of individual surrogate components, fuel volatilization, and the structural similarity of surrogate component fuels discouraged the examination of all component fuels. Toxicity issues are inherent to the combustion of aromatic fuels, such as surrogate components tetralin and *m*-xylene. The difficulties in volatilizing a heavy fuel such as tetradecane, coupled with its structural similarity to *n*-dodecane, have led to its elimination as a critical single component fuel. In view of these considerations, we chose to study *n*-dodecane, iso-octane, and methylcyclohexane flames as a prelude to the study of the surrogate. The use of these three fuels individually allows for the study of both well-known kinetic pathways, such as those for the oxidation of *n*-dode-

cane and iso-octane, and lesser known pathways, such as those for methylcyclohexane oxidation.

The results below are organized on the basis of fuel composition. For each surrogate component fuel, we study three flames of similar inlet composition and strain rate, and we present representative comparisons of predicted and measured temperature profiles and extinction limits for each case. Next, we examine two non-sooting counter-flow diffusion flames using the six-component surrogate blend, and we compare predicted temperature profiles and extinction limits for the surrogate blend with measurements in both a surrogate flame and a JP-8 flame at similar fuel flow rates. All calculations use the semi-detailed kinetic mechanism described above. The length of the computational domain corresponds to a burner separation of 1.25 cm, and the resulting computational grids contain approximately 250 adaptively determined grid nodes.

5.1. Temperature profiles for single-component flames

In Figs. 2–4, measured and predicted temperature profiles are presented as a function of distance from the fuel inlet for three individual surrogate component flames. For each of these three flames, the measured temperature profiles are slightly broader than the corresponding predicted profiles. This effect is expected, and it results from the intrusion of the thermocouple probe and its resulting perturbation of the velocity field. Furthermore, the predicted peak temperature for each flame is bracketed by the spherically

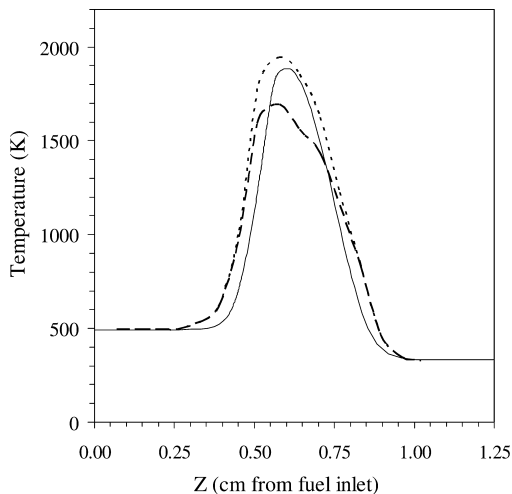


Fig. 2. Comparison of the predicted temperature profile [—] and the measured temperature profiles (cylindrical correction [---], spherical correction [—]) in a 1.52% *n*-dodecane/75% oxygen flame at a strain rate of 105 s^{-1} .

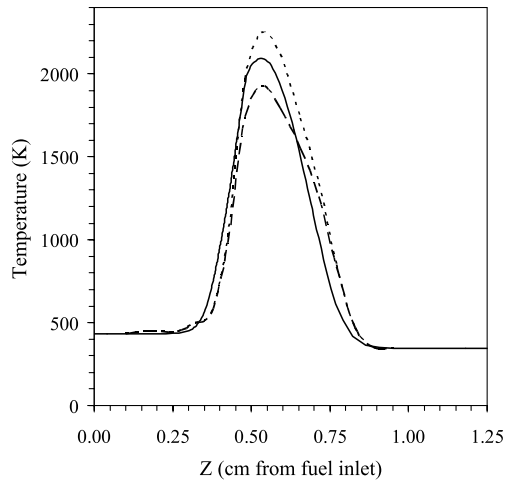


Fig. 3. Comparison of the predicted temperature profile [—] and the measured temperature profiles (cylindrical correction [---], spherical correction [—]) in a 2.91% iso-octane/77.4% oxygen flame at a strain rate of 110 s^{-1} .

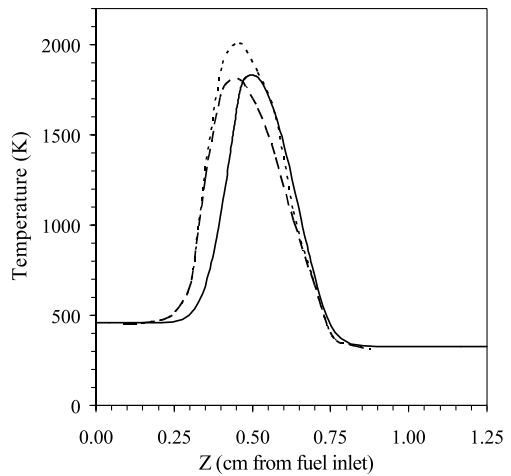


Fig. 4. Comparison of the predicted temperature profile [—] and the measured temperature profiles (cylindrical correction [---], spherical correction [—]) in a 2.44% methylcyclohexane/71.7% oxygen flame at a strain rate of 119 s^{-1} .

and cylindrically corrected measured profiles. This behavior results from uncertainty regarding the actual shape of the thermocouple probe, and the peak flame temperature is expected to reside somewhere between the two corrected values.

Temperature profiles for a 1.52% *n*-dodecane-inert/75% oxygen-inert flame, on a molar basis, are presented in Fig. 2 at a strain rate of 105 s^{-1} . The predicted peak temperature of 1889 K exhibits good agreement with the cylindrically corrected peak measurement of 1947 K.

However, there exists a substantial discrepancy between locations of peak temperature. The location of the predicted peak is shifted approximately 0.25 mm to the oxidizer side of the measured location.

Figure 3 presents a comparison of predicted and measured temperature profiles for a 2.91% iso-octane-inert/77.4% oxygen-inert flame at a strain rate of 110 s^{-1} . Trends similar to those of *n*-dodecane are observed, with the predicted peak temperature of 2093 K agreeing to within 150 K of both the spherically and the cylindrically corrected measurements. There also exists a negligible discrepancy between the locations of the predicted and measured peak temperatures.

A comparison of the predicted and measured temperature profiles for a 2.4% methylcyclohexane-inert/71.7% oxygen-inert flame is presented in Fig. 4 for a strain rate of 119 s^{-1} . Good agreement exists between prediction and measurements, with the predicted peak temperature of 1833 K varying from the spherically corrected value by less than 50 K. The location of the predicted peak temperature is shifted approximately 0.5 mm toward the oxidizer side of the measured peak. This observed shift is consistent with the direction of the shift in *n*-dodecane flames, but it is larger in magnitude.

The discrepancies between the predicted and measured peak temperatures could suggest possible problems with the chemical kinetic model or the counterflow flame model. To gauge the effect of kinetic errors in single-component flames, we have performed a sensitivity analysis for the temperature in a *n*-dodecane flame, and used the results of the analysis to probe the influence of kinetic errors on the temperature profile. The rate constants for the most important reaction of *n*-dodecane (namely the abstraction reaction, $\text{R} + \text{C}_{12}\text{H}_{26}$) and the most sensitive reactions in the mechanism (namely, $\text{H} + \text{O}_2 + \text{M} \Rightarrow \text{HO}_2 + \text{M}$ and $\text{O} + \text{OH} + \text{M} \Rightarrow \text{HO}_2 + \text{M}$, where M is a third-body collision partner) were doubled, and the resulting temperature profiles were compared to that obtained with unperturbed kinetics. These large kinetic modifications do not appreciably change the magnitude of the peak temperature for the *n*-dodecane flame (the increase in the HO_2 pathway results in an increase of 20 K) or the location of that peak temperature (the observed shift of 0.04 mm is within the computational precision). Thus, it appears that the discrepancies between predicted and measured temperature profiles in this *n*-dodecane flame are likely the result of factors other than kinetics, such as transport properties or boundary conditions.

In Fig. 5, the impact of the computational fuel inlet velocity boundary condition is examined for the same methylcyclohexane flame described above. Instead of applying the plug flow boundary condition, we impose an axial velocity gradi-

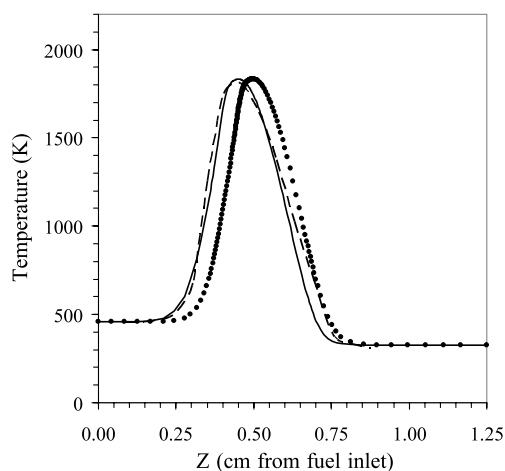


Fig. 5. Comparison of the measured temperature profile (spherically corrected [—]) with computed temperature profiles assuming a plug flow inlet velocity profile (●) and assuming an imposed fuel inlet velocity gradient [—] in a 2.4% methylcyclohexane/71.7% oxygen flame at a strain rate of 119 s^{-1} .

ent of 33 s^{-1} at the fuel inlet. The imposed gradient is equal in magnitude to that existing approximately 1.25 mm from the fuel inlet in the plug flow calculations of Fig. 4. In the resulting computed temperature profile (solid line in Fig. 5), the predicted peak is shifted towards the fuel inlet by roughly 0.5 mm. This predicted location, obtained with the imposed axial velocity gradient, is in excellent agreement with corrected measurements (dashed line in Fig. 5), thus demonstrating that details of the velocity boundary conditions can account for the discrepancy between the predicted and measured locations of peak temperature.

5.2. Extinction limits for single-component flames

The level of agreement that exists between the predicted and measured temperature profiles is encouraging, but in itself is not sufficient. A potentially more sensitive global observable for validation purposes is the extinction limit. Therefore, a comparison of predicted and measured extinction limits for each single-component flame is presented in Table 1. Although the selection of the path to extinction is a matter of choice, the present one, reached by gradually replacing the oxygen with inert in the oxidizer stream, has been motivated by the relatively restrictive conditions on the fuel side, both in terms of total liquid flow rate of the atomizer and of issues related to the complete volatilization of the stream.

Predicted extinction limits, reported in oxygen mole fraction, are lower than their corresponding measured extinction limits for each single-compo-

Table 1
Predicted and measured extinction limits for single-component and six-component surrogate flames

Fuel	Strain rate (s ⁻¹)	X _F	X _{O₂}	Predicted limit (X _{O₂})	Measured limit (X _{O₂})	Variation (%)
Surrogate/JP-8	115	0.02	0.77	0.55	0.59	6.78
	95	0.01	0.77	0.62	0.60	3.33
<i>n</i> -Dodecane (C ₁₂ H ₂₆)	72	0.02	0.66	0.26	0.31	16.13
	105	0.02	0.75	0.33	0.37	10.80
	102	0.01	0.75	0.38	0.43	11.63
Methylcyclohexane (C ₇ H ₁₄)	129	0.03	0.46	0.28	0.34	17.64
	119	0.02	0.72	0.35	0.39	7.89
	147	0.03	0.55	0.34	0.41	17.07
Iso-octane (C ₈ H ₁₈)	151	0.03	0.63	0.34	0.36	5.56
	123	0.02	0.81	0.41	0.44	6.82
	110	0.03	0.77	0.30	0.34	11.76

ment flame presented in Table 1. For *n*-dodecane flames, predicted extinction limits agree to within 16% of measurement. The level of agreement is somewhat worse in methylcyclohexane flames, with predictions falling within 18% of measurement, and it is somewhat better for iso-octane flames, as predictions agree to within either 6.8% or 12% of measurement. These results, especially those for iso-octane flames, are comparable to those observed in extinction studies examining much simpler fuels [19]. In passing, we note that these levels of agreement may be affected by the method used to vaporize the liquid fuel. For the current study, iso-octane has been vaporized through the use of an ultrasonic nebulizer, while *n*-dodecane and methylcyclohexane have been vaporized through the use of a bubbler/saturator. The nebulizer enables finer control over the inlet fuel mass flow, resulting in better agreement between predicted and measured extinction limits as seen in Table 1.

5.3. Temperature profiles for six-component surrogate flames

Experimentally, we examine both surrogate flames and JP-8 flames at similar flow rates and compare measured temperatures to predictions obtained using the surrogate model. This allows for the validation of the kinetic mechanism using the surrogate blend, while at the same time indicating the degree to which the six-component surrogate mimics the flame structure of the analogous JP-8 flame. As expected, and as discussed in Section 5.1, the predicted temperature profiles for the surrogate flames are slightly narrower than the measured profiles, and their peak values are bracketed by both sets of the cylindrically and spherically corrected measurements.

The predicted temperature profile for a 1.6% surrogate-inert/76.8% oxygen-inert flame is presented in Fig. 6 at a strain rate of 115 s⁻¹.

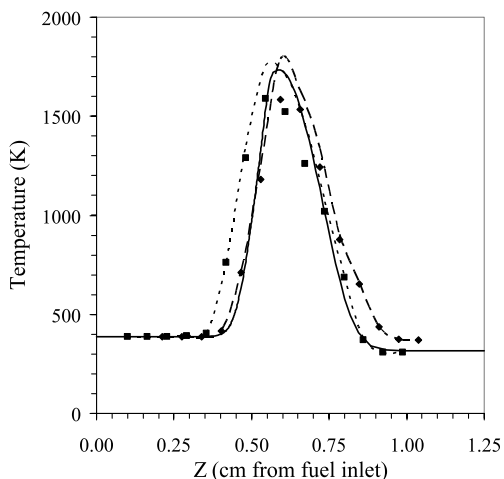


Fig. 6. Comparison of the predicted temperature profile [—] for a surrogate flame and measured profiles for a comparable surrogate flame (cylindrical correction [---], spherical correction [■]) and a JP-8 flame (cylindrical correction [---], spherical correction [◆]). Predictions and measurements correspond to a 1.6% surrogate/76.8% oxygen flame at a strain rate of 115 s⁻¹.

The peak measured temperatures for the JP-8 and the surrogate flames are quite similar, and both fall within 100 K of the predicted peak temperature. The measured temperature profiles are separated by approximately 0.5 mm, with the measured surrogate profile residing on the fuel side of the measured JP-8 profile. The width of the predicted temperature profile and the predicted peak temperature location exhibit better agreement with measurements in JP-8 flames than that exhibited between predictions and measurements in surrogate flames.

In Fig. 7, we present a comparison for a second surrogate flame with a similar inlet composition (1.4% surrogate-inert/76.8% oxygen-inert) and a slightly lower strain rate of 95 s⁻¹. No shift is

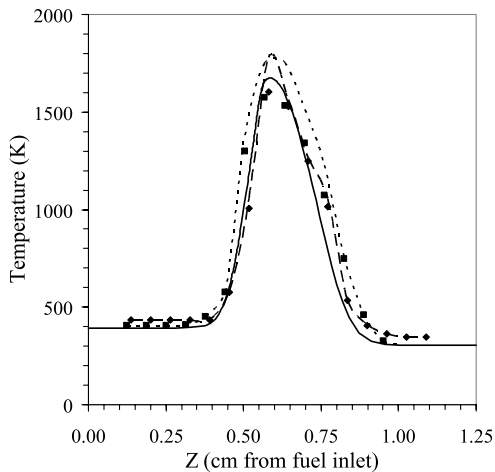


Fig. 7. Comparison of the predicted temperature profile [—] for a surrogate flame and measured profiles for a comparable surrogate flame (cylindrical correction [---], spherical correction [■]) and a JP-8 flame (cylindrical correction [—], spherical correction [◆]). Predictions and measurements correspond to a 1.4% surrogate/76.8% oxygen flame at a strain rate of 95 s^{-1} .

observed between the measured temperature profiles for the surrogate flame and the JP-8 flame, although a mildly non-monotonic temperature decrease is measured in the case of the JP-8 flame on the oxidizer side of the peak. This behavior is attributable to the intrusiveness of the thermocouple probe into the velocity field. The location and the magnitude of the predicted peak temperature exhibit very good agreement with measurements in both JP-8 flames and surrogate flames, better than in the case of the individual components. Also, in this case, the shape of the predicted temperature profile best agrees with the shape of the measured profile for the JP-8 flame, especially in the high temperature region above 1200 K.

5.4. Extinction limits for JP-8 surrogate flames

A comparison of predicted and measured extinction limits is presented in Table 1 for two surrogate flames of similar composition and strain rate. The notation is obvious, except for the third and fourth columns, showing the fuel and oxygen mole fractions, respectively. The extinction limits for surrogate flames and for JP-8 flames have been measured at comparable fuel mass flow rates and have been found to be virtually indistinguishable. For this reason, only one set of measured limits is presented for each flame. The predicted extinction limit underestimates the corresponding measured value for the higher-strain flame, while it overestimates it in the lower-strain case. However, these predicted limits agree to within 7% and 3%, respectively, of measurements. This level of agree-

ment is comparable, and in some cases, superior to that observed in many extinction studies using simpler fuels, such as methane, and simpler chemistry [18,19]. Although these results are encouraging, an examination of more sensitive indicators of mechanism validity, such as species concentration measurements, is necessary to characterize better the nature of this observed agreement, and examine the possibility of fortuitous cancellation in the complex kinetic scheme.

6. Conclusions

Counterflow diffusion flames using JP-8, a six-component JP-8 surrogate, and individual surrogate components have been investigated both computationally and experimentally. We note reasonably good agreement between predicted and measured temperature profiles and extinction limits in single-component *n*-dodecane, iso-octane, and methylcyclohexane flames. We also observe a shift between the predicted and measured locations of peak temperature. Inaccuracies in the chemical kinetic model and, more likely, in the computational inlet velocity boundary conditions are potential culprits for this discrepancy.

Good agreement is also observed in the comparison of temperature profiles and extinction limits in surrogate flames. The agreement is even better in the case of JP-8 flames. Notably, the extinction limits for the surrogate and JP-8 were found to be virtually undistinguishable.

Acknowledgments

The authors gratefully acknowledge the support of DARPA, under Grant No. DAAD19-01-1-0664 (Dr. R. J. Paur, Contract Monitor), and the Sandia National Laboratories under the Yale University Excellence in Engineering Fellowship. The technical assistance of Mr. N. Bernardo in the construction of the hardware is also gratefully acknowledged.

References

- [1] R.W. Bilger, *Combust. Sci. Technol.* 98 (1994) 223–228.
- [2] P. Dagaut, M. Reuillon, J.-C. Boettner, M. Cathonnet, *Proc. Combust. Inst.* 25 (1994) 919–926.
- [3] P.M. Patterson, A.G. Kyne, M. Pourkashanian, A. Williams, *J. Prop. Power* 16 (2) (2000) 453–460.
- [4] P. Dagaut, *Phys. Chem. Chem. Phys.* 4 (11) (2002) 2079–2094.
- [5] C. Douté, J.L. Delfau, R. Akrich, C. Vovelle, *Combust. Sci. Technol.* 106 (4–6) (1995) 327–344.
- [6] R.P. Lindstedt, L.Q. Maurice, *J. Prop. Power* 16 (2) (2000) 187–195.

- [7] J.A. Cooke, M.D. Smooke, M. Bellucci, A. Gomez, A. Violi, T. Faravelli, E. Ranzi, in: *Proceedings of the Third Joint Meeting of the US Sections of The Combustion Institute*. Eastern States, Central States, and Western States Sections of The Combustion Institute, Chicago, IL, 2003.
- [8] A. Violi, S. Yan, E.G. Eddings, A.F. Sarofim, S. Granata, T. Faravelli, E. Ranzi, *Combust. Sci. Technol.* 174 (11–12) (2002) 399–417.
- [9] E. Ranzi, M. Dente, G. Bozzano, A. Goldaniga, T. Faravelli, *Prog. Energ. Combust. Sci.* 27 (2001) 99–139.
- [10] M.D. Smooke, V. Giovangigli, *Proc. Combust. Inst.* 24 (1992) 161–168.
- [11] V. Giovangigli, N. Darabiha, in: C.M. Brauner, C. Schmidt-Lainé (Eds.), *Mathematical Modeling in Combustion and Related Topics*. Nijhoff, Dordrecht, 1988, p. 491.
- [12] R.J. Hall, *J. Quant. Spec. Rad. Trans.* 49 (5) (1995) 517–523.
- [13] M.D. Smooke, J.A. Miller, R.J. Kee, *Combust. Sci. Technol.* 34 (1–6) (1983) 79–84.
- [14] M.D. Smooke, I.K. Puri, K. Seshadri, *Proc. Combust. Inst.* 21 (1988) 1783–1792.
- [15] M.D. Smooke, *J. Comput. Phys.* 48 (1) (1982) 72–105.
- [16] V. Giovangigli, M.D. Smooke, *Appl. Numer. Math.* 5 (4) (1989) 305–330.
- [17] H.B. Keller, in: P. Rabinovitch (Ed.), *Applications of Bifurcation Theory*. Academic Press, San Diego, CA, 1977, p. 359.
- [18] H.K. Chelliah, C.K. Law, T. Ueda, M.D. Smooke, F.A. Williams, *Proc. Combust. Inst.* 23 (1990) 503–511.
- [19] M.D. Smooke, K. Seshadri, I.K. Puri, *Proc. Combust. Inst.* 22 (1988) 1555–1563.

Comment

Jim Quintiere, University of Maryland, USA. In your JP-8 surrogate temperature measurements, you show a displacement between the corrected spherical and cylindrical thermocouple measurements. Could you comment on your correction analysis vis-à-vis radiation emissivity values and wire conduction? Why might this displacement occur?

Reply. There is no noticeable displacement between the spherically and cylindrically corrected temperature measurements, nor should such a displacement exist. The intrusion of the thermocouple bead (0.2 mm in diameter) into the velocity field and the resulting perturbation of that field could result in a displacement of the flame on the order of the thermocouple bead size. This effect could account for relatively small displacements between measurements and calculations observed in *n*-dodecane, iso-octane, and JP-8 surrogate flames, but cannot alone resolve the largest displacements (up to 0.5 mm in magnitude) observed most notably in methylcyclohexane flames.

The uncertainties associated with the use of the thermocouples in flames are known and have been well docu-

mented in the literature [1]. The thermocouple probes were coated with silica (SiO₂) to minimize catalytic effects, and they were monitored and replaced frequently when cracks in the silica coating were observed. By aligning the thermocouple probe in a plane parallel to the flame, we took advantage of the flatness of the temperature profile in the radial direction to minimize the effects wire conduction in the thermocouple probe. Temperature corrections were made on the basis of only a convective-radiative balance and used a geometry-dependent correlation for the Nusselt number. Calculations were performed using both a cylindrical and a spherical geometry, as the actual shape of the thermocouple bead tends to be somewhat irregular and may be approximated by an ellipsoid. As a result, the corrections are likely to bracket the true gas temperature. The correction used a value for the emissivity of silica-coated thermocouples [2].

References

- [1] R.M. Fristom, *Flame Structure and Processes*, Oxford University Press, New York, 1995, p. 119.
- [2] W.E. Kaskan, *Proc. Comb. Inst.* 6 (1957) 134–143.